Applications of Micro Phasor Measurement Units for Enhancing Situational Awareness in Smart Power Distribution Networks: An Integrated Part of Smart City

Santoshkumar Hampannavar[1*], *Deepa* Bobbakunte[2], *Swapana* Mansani[3]

[1]Director, BTKIT, Dwarahat, India.
[2]Electrical and Electronics Engineering, RYMEC, Ballari, India.
3Department of Electrical Engineering, National Institute of technology, Silchar, India.

Abstract. Smart cities require reliable and intelligent power infrastructure to ensure efficient energy management and sustainability. Smart Grid (SG) technology integrates Information and Communication Technology (ICT), advanced sensors, and control systems to enable real-time monitoring and improved situational awareness. In this paper, optimal placement of micro phasor measurement units using a General Algebraic Modeling System (GAMS)-based Mixed Integer Linear Programming (MILP) approach is proposed for the IEEE 33-bus distribution system. The study also investigates the impact of Electric Vehicle Charging Stations (EVCSs) and Distributed Generators (DGs) under different operating scenarios. The results demonstrate improved voltage observability, enhanced voltage profile, reduced power losses, and lower execution time compared to conventional monitoring methods. Simulations were carried out using GAMS and MATLAB

1 Introduction

Rapid urbanization, population growth, and increasing energy demand have accelerated the development of smart cities across the world. Smart cities aim to improve the quality of life by efficiently managing infrastructure, transportation, communication systems, water resources, healthcare, and energy utilization while minimizing environmental impact and greenhouse gas emissions [1]. The growing demand for sustainable energy management has encouraged researchers and policymakers to adopt intelligent technologies capable of improving operational efficiency and resource utilization in urban environments [2].

Among various smart city infrastructures, the electrical power system plays a crucial role in ensuring reliability, sustainability, and uninterrupted energy supply. Conventional power systems face several challenges such as increasing electricity demand, integration of renewable energy resources, aging infrastructure, and operational inefficiencies. To overcome these limitations, Smart Grid (SG) technology has emerged as an advanced solution integrating Information and Communication Technology (ICT), intelligent sensors, automation, and real-time communication systems into conventional electrical networks [3]. Smart grids improve power system reliability, operational flexibility, monitoring capability, and energy efficiency through bidirectional communication between utilities and consumers.

According to United Nations estimates, the urban population is expected to increase significantly by 2050, especially in developing countries across Asia and Africa [4-5]. Urban regions currently consume a major portion of global electricity production and contribute substantially to greenhouse gas emissions. Consequently, efficient energy management and intelligent power system operation have become essential requirements for future smart city development. The integration of Renewable Energy Sources (RESs), Electric Vehicles (EVs), and Plug-in Hybrid Electric Vehicles (PHEVs) into modern power systems further increases the complexity of distribution network operation and monitoring [6-7].

1.1 Role of Smart Grid in a Smart City

Traditional power distribution systems are primarily designed for unidirectional power flow from centralized generation stations to consumers and offer limited communication capability [8]. In contrast, smart grids utilize ICT infrastructure, advanced metering systems, communication technologies, and automation devices to enable real-time bidirectional information exchange among system components [9]. Smart grids support intelligent monitoring, demand response, distributed generation integration, self-healing capability, and automated control operations [10].

* Corresponding author: santoshkumar777@yahoo.com

The increasing adoption of EVs and renewable generation systems has introduced additional operational challenges such as voltage fluctuations, increased loading conditions, and power quality issues in distribution networks. Smart grids address these challenges through intelligent communication systems and advanced monitoring technologies capable of providing real-time situational awareness and operational control [11-12]. Technologies such as smart substations, smart meters, Supervisory Control and Data Acquisition (SCADA) systems, and Phasor Measurement Units (PMUs) significantly improve monitoring and automation capabilities in modern power systems.

PMUs provide synchronized voltage and current phasor measurements with high sampling accuracy and time synchronization using Global Positioning System (GPS) signals. Compared to conventional monitoring systems, PMU-based monitoring enables operators to perform real-time analysis, fault detection, and corrective control actions within milliseconds, thereby improving grid reliability and stability [13].

1.2 Phasor Measurement Units

Phasor Measurement Units (PMUs) have become one of the most important monitoring devices in smart grid applications due to their ability to provide synchronized measurements over geographically distributed power networks. PMUs form the backbone of Wide Area Measurement Systems (WAMS) and provide real-time situational awareness for interconnected transmission and distribution systems. The deployment of PMUs significantly improves observability, state estimation accuracy, dynamic monitoring capability, and disturbance analysis in modern power systems.

The increasing penetration of Distributed Energy Resources (DERs), distributed generation, and EV charging infrastructure has created a strong need for advanced monitoring and protection of active distribution systems. Traditionally, distribution systems were designed only to transfer power from centralized generating stations to end consumers. However, modern active distribution networks require continuous operational monitoring and control due to the bidirectional nature of power flow introduced by DER integration.

Several state estimation and phasor estimation techniques have been proposed for PMU applications in power systems. Discrete Fourier Transform (DFT)-based methods are widely used due to their simplicity and harmonic rejection capability. However, several existing methods still face challenges related to interference rejection, off-nominal frequency operation, and computational complexity[14-15]. Although PMUs are extensively utilized in transmission networks, distribution systems present additional challenges due to short electrical distances, low voltage magnitudes, large number of nodes, and small phase angle variations between buses.

To address these limitations, micro-Phasor Measurement Units (μPMUs) have been introduced for distribution-level situational awareness and real-time monitoring applications. Optimal placement of μPMUs is essential for maximizing system observability while minimizing installation cost and computational burden. Existing studies have investigated PMU placement using optimization techniques such as Genetic Algorithms (GA), Particle Swarm Optimization (PSO), and Integer Linear Programming (ILP). However, limited research has focused on General Algebraic Modeling System (GAMS)-based Mixed Integer Linear Programming (MILP) approaches for optimal μPMU placement considering integrated Electric Vehicle Charging Stations (EVCSs) and Distributed Generators (DGs) in active distribution networks.

Therefore, this work proposes a GAMS-based MILP framework for optimal μPMU placement in the IEEE 33-bus distribution system. The proposed study further investigates the impact of EVCSs and DG operating scenarios on voltage observability, voltage profile improvement, and system performance using PLL-based μPMU measurements and forward/backward sweep power flow analysis.

1.3 Related Work and Research Gap

Several optimization techniques have been proposed in the literature for optimal PMU and μPMU placement in power systems. Existing methods include Genetic Algorithm (GA), Binary Particle Swarm Optimization (BPSO), Integer Linear Programming (ILP), heuristic optimization techniques, and graph-theory-based approaches. GA-based techniques provide acceptable observability solutions but often require higher computational effort and longer convergence time for large-scale systems. BPSO methods improve convergence characteristics; however, they may converge to locally optimal solutions under complex operating constraints. ILP-based approaches provide mathematically optimal placement solutions but their implementation complexity increases with network size and operational scenarios.

Recent research has focused on improving distribution system observability due to increasing integration of Distributed Energy Resources (DERs), Electric Vehicle Charging Stations (EVCSs), renewable energy systems, and Distributed Generators (DGs). Several studies have investigated PMU-based state estimation, voltage stability monitoring, power quality assessment, and situational awareness enhancement in active distribution networks. However, most existing works primarily focus on transmission-level applications or conventional PMU placement methods without considering integrated EVCS and DG operating scenarios in smart distribution systems.

Furthermore, only limited studies have investigated General Algebraic Modeling System (GAMS)-based Mixed Integer Linear Programming (MILP) approaches for optimal μPMU placement in the IEEE 33-bus distribution network. Comparative analysis between PLL-based μPMU monitoring and conventional monitoring techniques with respect to observability enhancement, voltage profile improvement, and execution time reduction is also insufficiently explored in the existing literature.

Therefore, this work proposes a GAMS-based MILP framework for optimal µPMU placement considering integrated EVCS and DG operating scenarios in the IEEE 33-bus smart distribution system. The proposed work focuses on improving voltage observability, reducing power losses, enhancing voltage profile performance, and evaluating monitoring execution time using PLL-based µPMU measurements and forward/backward sweep power flow analysis.

The major contributions of the proposed work are summarized as follows:

1. Integration and analysis of Electric Vehicle Charging Stations (EVCSs) and Distributed Generators (DGs) under multiple operating scenarios.
2. Comparative evaluation of PLL-based µPMU monitoring and conventional monitoring techniques.
3. Improvement of voltage observability, voltage profile performance, and reduction of system power losses.
4. Evaluation of computational efficiency and execution time for smart grid situational awareness applications.

2 Need for µpmus in the smart distribution network

Multiple nodes, low amplitude, short distances, and angle differences between nodes make distribution systems challenging. Devices must be added to the distribution network in order to do quick real-time measurements; as a result, distribution level D-PMU or micro-PMU (PMU) presents a new avenue for distribution network research. PMU monitors time-synchronized voltage and phase angles with better observability thanks to high sample rates of 30 samples per second for transmission and 120 samples per second for distribution. In a balanced transmission system, the observability of one bus translates into the observation of nearby buses. Conceptual view of µPMUs connected in distribution network is depicted in Fig. 1.

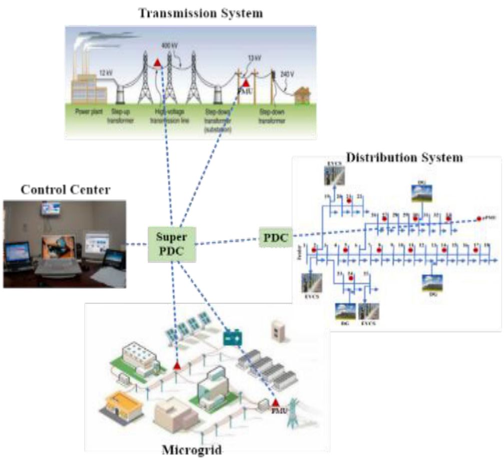

Fig. 1. Conceptual view of µPMUs connected in Smart Grid

The distribution network's PMU deployment must be done in a way that minimizes the distance between observed and unobserved buses in order to increase the power system's observability. When a power system's bus voltages cannot be fully determined by a PMU's number and position, this is referred to as incomplete observability. While buses A, C, and F can be computed using the measured voltages and currents, buses B and G are directly observed by PMU 1 and 2, respectively. Thus, PMU buses B and G are used to measure voltage and current directly. Depth-of-two unobservability (D & E) is shown in Fig. 2.

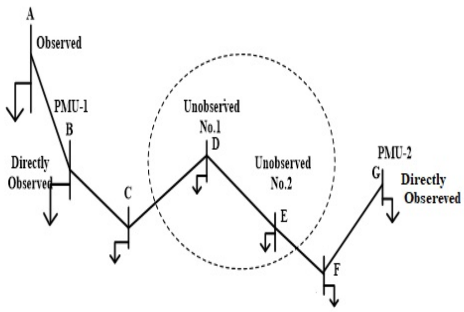

Fig. 2. Depth of two unobservability illustrated

3 Results and Discussion

For PMU placement in distribution network for full and maximum observability, simulations were carried out on an IEEE 33 bus. For analysis and evaluation, the General Algebraic Modeling System (GAMS) was employed because computation time is very less when compared to other methods. For different µPMUs, the number of buses observed are shown in Table 1. This study helps to determine the approximate number of µPMUs needed for a situational awareness wide area measuring system (WAMS) developed for distribution networks.

Table 1: Effective node positions for maximizing observability with minimal PMU deployment in the IEEE 33 bus system

Test System	Number of µPMUs	Node location	No. of buses observed	Buses observed
33	2	3,6	8	2,3,4,5,6,7,23,26
	4	3,6,9,20	14	2,3,4,5,6,7,8,9,10,19,20,21,23,26
	6	3,6,9,17,20,30	20	2,3,4,5,6,7,8,9,10,16,17,18,19,20,21,22,23,26,29,30,31
	8	2,6,9,13,17,21,24,30	26	1,2,3,5,6,7,8,9,10,12,13,14,16,17,18,19,20,21,22,23,24,25,26,29,30,31
	10	2,6,8,11,14,17,21,24,29,32	31	1,2,3,5,6,7,8,9,10,11,12,13,14,15,16,17,18,19,20,21,22,23,24,25,26,28,29,30,31,32,33
	11	2,5,8,11,14,17,21,24,27,30,33	33	1-33

3.1 Distribution system integrated with EVCS and DGs

Fig. 3 illustrates the line diagram of the 33 bus test system with integrated EVCS and DGs. As mentioned in the previous section, the distribution network test system's PMUs are deployed according to the outcomes of the most optimal PMU locations. It has been noted that the outcomes of PLL-based μPMU measurements closely resemble the outcomes of the forward-backward sweep technique.

This article categorically examines how EVCSs and DGs affect bus voltage and system losses using type 1 and type 2 DGs.

Type-1 only injects active power to the system.

Type-2 injects both active and reactive power.

In this research, the following summaries are provided:

Scenario 1: IEEE 33 bus system without EVCS and without integrating DGs (Base Case).

The IEEE 33 bus system is taken into consideration without EVCS and DGs. All test systems have a base MVA of 100 and a rated line voltage of 12.66 kV. The total real and reactive demand of the system is 2.3MVar and 3.715MW. The system's total active and reactive power losses are 0.19061 MW and 0.14123 MVAr, respectively.

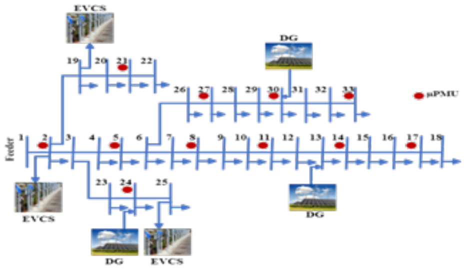

Fig. 3. IEEE 33 bus system integrated with EVCS and DG

Scenario 2: IEEE 33 bus system with EVCS load and without integrating DGs.

It is envisaged that three EVCSs will be loaded into the system overall. The test system's new loading condition is established by placing three EVCSs under a total power demand of 2925kW (975kW×3). This results in an increase in the active power load from 3715kW to 6640kW. The related test system performance with and without reactive power support is given in Table 2. With the EVCS reactive power support losses are reduced to considerable extent. Table 3 shows the voltage magnitudes achieved with and without EVCS reactive aid using the forward/backward sweep power flow method. The EVCS reactive power support also enhances the voltage magnitudes. Table 4 demonstrates a clear improvement in the observability of voltage magnitudes from PMUs as compared to the forward/backward sweep power flow method.

Table 2. Performance of IEEE 33 bus system with EVCS at optimal locations without integrating DGs

Scenarios	Bus number and size	EVCS without Reactive power support		EVCS with Reactive power support	
		Active Power loss (MW)	**Reactive Power loss (MVar)**	**Active Power loss (MW)**	**Reactive Power loss (MVar)**
Base Case	---	0.19061	0.14123	0.19061	0.14123
1 EVCS	975 kW at bus 2	0.19578	0.14393	0.193801	0.14289
2 EVCS	975 kW at bus 2 and bus 19	0.20382	0.14884	0.20095	0.14381
3 EVCS	975 kW at bus 2, bus 19 and bus 25	0.27459	0.19431	0.261835	0.18773

Table 3. Voltage magnitudes obtained from forward/backward sweep algorithm

		Voltage magnitude (p.u) integrating EVCS without Reactive power support			Voltage magnitude (p.u) integrating EVCS with Reactive power support		
Bus No.	**Base Case**	**1 EVCS 975 kW at bus 2**	**2 EVCS 975 kW at bus 2 and 19**	**3 EVCS 975 kW at bus 2, 19 and 25**	**1 EVCS 975 kW/700KVar at bus 2**	**2 EVCS 975 kW/700KVar at bus 2 and 19**	**3 EVCS 975 kW/700KVar at bus 2, 19 and 25**
2	1	0.9994	0.9989	0.9983	0.9996	0.9993	0.9989
5	0.9760	0.9754	0.9748	0.9709	0.9756	0.9752	0.9727
8	0.9405	0.9399	0.9392	0.9351	0.9401	0.9397	0.9370
11	0.9274	0.9268	0.9262	0.9221	0.9271	0.9267	0.9240
14	0.9175	0.9169	0.9163	0.9121	0.9171	0.9167	0.9140
17	0.9127	0.9121	0.9114	0.9072	0.9123	0.9119	0.9091
21	0.9952	0.9946	0.9930	0.9924	0.9948	0.9941	0.9937
24	0.9756	0.9750	0.9745	0.9616	0.9753	0.9749	0.9681
27	0.9531	0.9525	0.9519	0.9478	0.9527	0.9523	0.9497
30	0.9300	0.9294	0.9287	0.9246	0.9296	0.9292	0.9265
33	0.9246	0.9240	0.9234	0.9192	0.9242	0.9238	0.9211

Table 4. Voltage magnitudes obtained from PMUs

		Voltage magnitude (p.u) integrating EVCS without Reactive power support			Voltage magnitude (p.u) integrating EVCS with Reactive power support		
Bus No.	**Base Case**	**1 EVCS 975 kW at bus 2**	**2 EVCS 975 kW at bus 2 and 19**	**3 EVCS 975 kW at bus 2,v19 and 25**	**1 EVCS 975 kW/700KVar at bus 2**	**2 EVCS 975 kW/700KVar at bus 2 and 19**	**3 EVCS 975 kW/700KVar at bus 2, 19 and 25**
2	0.9973	0.9997	0.9962	0.9956	1	1	1
5	0.9759	0.9753	0.9748	0.9715	0.9785	0.9785	0.9826
8	0.945	0.9445	0.9439	0.9407	0.9476	0.9476	0.9515
11	0.9339	0.9334	0.9328	0.9297	0.9364	0.9364	0.9404
14	0.9255	0.925	0.9244	0.9213	0.928	0.928	0.9313
17	0.9214	0.9209	0.9204	0.9172	0.9239	0.9239	0.9278
21	0.9925	0.992	0.9904	0.9899	0.9952	0.9957	0.9957
24	0.9748	0.9743	0.9737	0.9626	0.9775	0.9775	0.9945
27	0.9559	0.9553	0.9548	0.9516	0.9585	0.9585	0.9625
30	0.9358	0.9353	0.9347	0.9316	0.9383	0.9383	0.9423
33	0.9312	0.9307	0.9301	0.927	0.9337	0.9337	0.9376

Scenario 3: IEEE 33 bus system with EVCS load with reactive power support and Type 1 DG

It is assumed that three EVCSs with reactive power assistance will be integrated with real power at the best possible places in the test system (buses 2, 19, and 25). The positioning of numerous DGs has a major effect on a power system's voltage profile. Table 5 shows the voltage magnitudes obtained by the forward/backward sweep power flow approach. while the voltage magnitudes acquired from PMUs are displayed in Table 6. It is clear from Table 7 that the observability of voltage magnitudes from PMUs has significantly improved. The integration of DGs greatly improves all node voltages, which fall within the permitted range of +5%.

Table 5: Voltage magnitudes obtained from forward/backward sweep algorithm

Type-1				Voltage magnitude (p.u) by injecting only Real power			
Bus No.	**Base Case**	**1 EVCS 975 kW at bus 2**	**2 EVCS 975 kW at bus 2 and 19**	**3 EVCS 975 kW at bus 2, 19 and 25**	**1 DG with 2589.6 kw at bus 6**	**2 DGs with 1898.7 kw at bus 6 649.9 kw at bus 14**	**3 DGs with 790 kw at bus 13 107 kw at bus 24 101 kw at bus 30**
2	1	0.9996	0.9993	0.9989	1.0005	1.0005	1.0008
5	0.9760	0.9756	0.9752	0.9727	0.9898	0.9897	0.9894
8	0.9405	0.9401	0.9397	0.9370	0.9688	0.9769	0.9745
11	0.9274	0.9271	0.9267	0.9240	0.9562	0.9741	0.9736
14	0.9175	0.9171	0.9167	0.9140	0.9465	0.9747	0.9736
17	0.9127	0.9123	0.9119	0.9091	0.9418	0.9701	0.9690
21	0.9952	0.9948	0.9941	0.9937	0.9953	0.9953	0.9957
24	0.9756	0.9753	0.9749	0.9681	0.9782	0.9782	0.9898
27	0.9531	0.9527	0.9523	0.9497	0.9810	0.9809	0.9800
30	0.9300	0.9296	0.9292	0.9265	0.9586	0.9585	0.9732
33	0.9246	0.9242	0.9238	0.9211	0.9534	0.9533	0.9681

Table 6: Voltage magnitude results obtained from PMU

Type-1	Voltage magnitude (p.u) by injecting only Real power						
Bus No.	**Base Case**	**1 EVCS 975 kW at bus 2**	**2 EVCS 975 kW at bus 2 and 19**	**3 EVCS 975 kW at bus 2, 19 and 25**	**1 DG with 2589.6 kw at bus 6**	**2 DGs with 1898.7 kw at bus 6 649.9 kw at bus 14**	**3 DGs with 790 kw at bus 13 107 kw at bus 24 101 kw at bus 30**
2	0.9973	1	1	1	1	1	1
5	0.9759	0.9785	0.9785	0.9826	0.9989	0.9989	0.9968
8	0.945	0.9476	0.9476	0.9515	0.9846	0.9954	0.9974
11	0.9339	0.9364	0.9364	0.9404	0.973	0.9956	0.9951
14	0.9255	0.928	0.928	0.9313	0.9642	1	0.9979
17	0.9214	0.9239	0.9239	0.9278	0.96	0.9956	0.9935
21	0.9925	0.9952	0.9957	0.9957	0.9957	0.9957	0.9957
24	0.9748	0.9775	0.9775	0.9945	0.9974	0.9974	1
27	0.9559	0.9585	0.9585	0.9625	0.9959	0.9959	0.9951
30	0.9358	0.9383	0.9383	0.9423	0.975	0.975	1
33	0.9312	0.9337	0.9337	0.9376	0.9702	0.9702	0.9951

Scenario 4: IEEE 33 bus system with EVCS load and Type 2 DG

It is envisaged that type 2 DG will integrate three EVCSs with reactive power supply. Multiple DGs minimize overall power losses by 55.25%, 63.9%, and 75.6%, respectively. Tables 7 and 8 display voltage magnitudes derived from PMUs and the forward/backward sweep approach. Table 8 shows that the PMU values are within the permitted range of +5% when DGs are included.

Table 7: Voltage magnitudes obtained from forward/backward sweep algorithm

Type-1	Voltage magnitude (p.u) by injecting Active and Reactive power						
Bus No.	**Base Case**	**1 EVCS 975 kW at bus 2**	**2 EVCS 975 kW at bus 2 and 19**	**3 EVCS 975 kW at bus 2, 19 and 25**	**1 DG with 2589.6 kw at bus 6**	**2 DGs with 1898.7 kw at bus 6 649.9 kw at bus 14**	**3 DGs with 790 kw at bus 13 107 kw at bus 24 101 kw at bus 30**
2	1	0.9996	0.9993	0.9989	1.0010	1.0009	1.0012
5	0.9760	0.9756	0.9752	0.9727	0.9974	0.9962	0.9952
8	0.9405	0.9401	0.9397	0.9370	0.9844	0.9989	0.9895
11	0.9274	0.9271	0.9267	0.9240	0.9720	1.0052	0.9909
14	0.9175	0.9171	0.9167	0.9140	0.9625	0.9961	0.9927
17	0.9127	0.9123	0.9119	0.9091	0.9579	0.9916	0.9883
21	0.9952	0.9948	0.9941	0.9937	0.9958	0.9957	0.9960
24	0.9756	0.9753	0.9749	0.9681	0.9816	0.9808	0.9974
27	0.9531	0.9527	0.9523	0.9497	0.9964	1.0005	0.9922
30	0.9300	0.9296	0.9292	0.9265	0.9744	1.0148	0.9949
33	0.9246	0.9242	0.9238	0.9211	0.9693	1.0099	0.9899

Table 8: Voltage magnitude results obtained from PMU

Type-1	Voltage magnitude (p.u) by injecting Active and Reactive power						
Bus No.	**Base Case**	**1 EVCS 975 kW at bus 2**	**2 EVCS 975 kW at bus 2 and 19**	**3 EVCS 975 kW at bus 2, 19 and 25**	**1 DG with 2589.6 kw at bus 6**	**2 DGs with 1898.7 kw at bus 6 649.9 kw at bus 14**	**3 DGs with 790 kw at bus 13 107 kw at bus 24 101 kw at bus 30**
2	0.9973	1	1	1	1	1	1
5	0.9759	0.9785	0.9785	0.9826	0.9989	0.9967	0.9968
8	0.945	0.9476	0.9476	0.9515	0.9846	0.9951	0.9924
11	0.9339	0.9364	0.9364	0.9404	0.973	1	0.9951
14	0.9255	0.928	0.928	0.9313	0.9642	0.991	0.9979
17	0.9214	0.9239	0.9239	0.9278	0.96	0.9866	0.9935

21	0.9925	0.9952	0.9957	0.9957	0.9957	0.9957	0.9957
24	0.9748	0.9775	0.9775	0.9945	0.9974	0.997	1
27	0.9559	0.9585	0.9585	0.9625	0.9959	0.9956	0.9951
30	0.9358	0.9383	0.9383	0.9423	0.975	1	1
33	0.9312	0.9337	0.9337	0.9376	0.9702	0.9951	0.9951

Table 9 shows the total power losses by integrating different types of DGs and EVCS with and without reactive power support and also percentage of reduction in losses for each case. From the studies it is evident that out of 2 cases, type 2 DGs which inject real and reactive power will reduce more power losses when compared to type 1 DG connection. Integration of renewable DG units plays significant role in economic, environmental and sustainable operation of a power system.

Table 9 : Comparison of Total Power losses by integrating different types of DGs

	Installed capacity of DG	EVCS without Reactive power support			EVCS with Reactive power support		
		Active power loss (MW)	**Reactive power loss (MVAr)**	**% Of loss reduction**	**Active power loss (MW)**	**Reactive power loss (MVAr)**	**% of loss reduction**
Base Case	----	0.19061	0.14123	----	0.19061	0.14123	----
1 EVCS	975 kW at bus 2	0.19578	0.14393	---	0.193801	0.14289	---
2 EVCS	975 kW at bus 2 and bus 19	0.20382	0.14884	---	0.20095	0.14381	---
3 EVCS	975 kW at bus 2, bus 19 and bus 25	0.27459	0.19431	---	0.261835	0.18773	---
Type 1							
1 DG	2589.6 kw at bus 6	0.16078	0.11992	41.44%	0.14896	0.11389	45.75%
2 DGs	1898.7 kw at bus 6 649.9 kw at bus 14	0.14121	0.10256	48.57%	0.129589	0.09667	52.8%
3 DGs	790 kw at bus 13 1070 kw at bus 24 1010 kw at bus 30	0.09893	0.07198	63.97%	0.08789	0.06647	67.98%
Type-2							
1 DG	2558.2kw/1761.1kvar at bus 6	0.12233	0.092437	55.44%	0.12287	0.09279	55.25%
2 DGs	1171.2kw/188.1kvar at bus 11 1095.4kw/1667.0kvar at bus 30	0.09763	0.06890	64.44%	0.09909	0.06971	63.9%
3 DGs	537.8kw/597.3kvar at bus 13 1058.9kw/832.9kvar at bus 24 967.7kw/832.6kvar at bus 30	0.05219	0.03769	80.99%	0.06699	0.04781	75.6%

The technical specifications of the computer used for simulations are an Intel 2.4-GHz CPU with 16 GB RAM.

4 CONCLUSION

With the Integration of DERs in smart grids, power system observability plays a crucial role in wide area monitoring to ensure complete system observability. In this paper, optimal placement of µPMU in the distribution network using GAMS is presented and it is implemented for IEEE 33 bus test system. The analysis further reveals that for complete observability of system using µPMU, the most accurate and the fastest among all the methods is MILP using GAMS for online/offline monitoring. Also, the system was comprehensively analysed and presented for different DGs with EVCS load. Injecting active power, injecting active/reactive power, and two distinct types for four scenarios were taken into consideration for the study. According to the data, type 2, which injects both actual and reactive power, significantly reduces power losses by up to 80.99%. A general-purpose Intel processor with 2.4 GHz and 16 GB of RAM was used to run the simulations. It was discovered that the minimum execution times for µPMUs and conventional monitoring were 5.64 seconds and 19.07 seconds, respectively. The execution time itself attests to the use of µPMUs for online control and monitoring. The suggested approach can be used for a number of power sector applications for security, smart grid setup, and decision-making. Presenting the state of the distribution network for situational awareness is beneficial. Network observability in the case of a single μPMU failure may be the subject of future studies.

References

1. M. Eremia, L. Toma and M. Sanduleac, The Smart City Concept in The 21st Century, *Procedia Engineering*, 181, 12-19, (2017).
2. M. Farmanbar, K. Parham, Ø. Arild and C. Rong, A Widespread Review of Smart Grids towards Smart Cities, *Energies*, 12(23), 4484, (2019).
3. O.S. Neffati, S. Sengan, K.D. Thangavelu, S. D.Kumar, R. Setiawan, M. Elangovan and P. Velayutham, Migrating From Traditional Grid to Smart Grid in Smart Cities Promoted in Developing Country, *Sustainable Energy Technologies and Assessments*, 45, 101125, (2021).
4. Santoshkumar Hampannavar, Suresh Chavhan, swapna Mansani, Udaykumar R. Yaragatti, Electrical vehicle traffic pattern analysis and prediction in aggregation regions/parking lot zones to support V2G operation in smart grid: A cyber-physical system entity, *International Journal of Emerging Electric Power Systems.* February (2020).
5. A. von Meier, D. Culler, A. McEachern, and R. Arghandeh, Micro-synchrophasors for distribution systems, *in Proc. IEEE Innov. Smart Grid Technol. Conf. (ISGT)*, Washington, DC, USA, Feb. (2014), pp. 1–5.
6. Mohammadi, Pooria, Shahab Mehraeen, and Hamidreza Nazaripouya. Sensitivity analysis-based optimal PMU placement for fault observability. IET Generation, Transmission & Distribution 15.4 (2021): 737-750.
7. Lin, Chenhui, Wenchuan Wu, and Ye Guo. Decentralized robust state estimation of active distribution grids incorporating microgrids based on PMU measurements. IEEE Transactions on Smart Grid 11.1 (2019): 810-820.
8. Rangu, Seshu Kumar, et al. Recent trends in power management strategies for optimal operation of distributed energy resources in microgrids: A comprehensive review. International Journal of Energy Research 44.13 (2020): 9889-9911.
9. H. Gharavi and B. Hu, Scalable synchrophasors communication network design and implementation for real-time distributed generation grid, *IEEE Trans. Smart Grid*, vol. 6, no. 5, pp. 2539–2550, Sep. (2015).
10. Sultana, U., et al. A review of optimum DG placement based on minimization of power losses and voltage stability enhancement of distribution system. Renewable and Sustainable Energy Reviews 63 (2016): 363-378.
11. Gou, Bei, and Rajesh G. Kavasseri. Unified PMU placement for observability and bad data detection in state estimation. IEEE Transactions on Power Systems 29.6 (2014): 2573-2580.
12. Y.-F. Huang, S. Werner, J. Huang, N. Kashyap, and V. Gupta, State estimation in electric power grids: Meeting new challenges presented by the requirements of the future grid, *IEEE Signal Process.* Mag., vol. 29, no. 5, pp. 33–43, Sep. 2012.
13. Vejdan, Sadegh, Majid Sanaye-Pasand, and Om P. Malik. Accurate dynamic phasor estimation based on the signal model under off-nominal frequency and oscillations. IEEE Transactions on Smart Grid 8.2 (2015): 708-719.
14. S. Hampannavar, C. B. Teja, M. Swapna and U. Kumar R.Y., Performance Improvement of M-Class Phasor Measurement Unit (PMU) using Hamming and Blackman Windows, 2020 *IEEE International Conference on Power Electronics, Smart Grid and Renewable Energy (PESGRE2020),* Cochin, India, 2020, pp. 1-5, doi: 10.1109/PESGRE45664.2020.9070382.
15. Giotopoulos, Vasilis, and Georgios Korres. Implementation of phasor measurement unit based on phase-locked loop techniques: A comprehensive review. Energies 16.14 (2023): 5465.